

## Supporting Information

### High-Power NIR-II LED of Nd<sup>3+</sup> Doped Glass Ceramic toward Portable Imaging

*Xiaodie Zhu,<sup>a, b #</sup>, Zhaowei Teng<sup>c #</sup>, Haitao Tang<sup>b #</sup>, Chao Wang<sup>b</sup>, Ya Liu<sup>b</sup>, Songcheng Peng<sup>b</sup>,*

*Zhichao Liu<sup>b</sup>, Shiwen Zhang<sup>d</sup>, Sibao Liu<sup>e</sup>, Xuhui Xu<sup>b \*</sup> and Xue Yu<sup>a \*</sup>*

a School of Mechanical Engineering, Institute for Advanced Materials Deformation and Damage from Multi-Scale, Chengdu University, Chengdu 610106, Sichuan, China

b Faculty of Materials Science and Engineering, Key Laboratory of Advanced Materials of Yunnan Province, Kunming University of Science and Technology, Kunming 650093, Yunnan, China

c The Central Laboratory and Department of orthopedic, The Second Affiliated Hospital of Kunming Medical University, Kunming, 650106, Yunnan, China; Clinical Medical Research Center and Key Laboratory of Yunnan Provincial Innovative Application of Traditional Chinese Medicine, The First Peoples Hospital of Yunnan Province, Affiliated Hospital of Kunming University of Science and Technology, Kunming, 650034, Yunnan, China

d The Head and Neck Surgery Department, The Third Affiliated Hospital of Kunming Medical University (Yunnan Cancer Hospital), Kunming 650118, Yunnan, China

e The Affiliated Hospital of Kunming University of Science and Technology, The First People's Hospital of Yunnan Province, Kunming 650031, Yunnan, China

\*Corresponding Author:

Xuhui Xu, E-mails: xuxuh07@126.com;

Xue Yu, E-mails: yuyu6593@126.com;

# These authors contributed equally: Xiaodie Zhu, Zhaowei Teng and Haitao Tang.

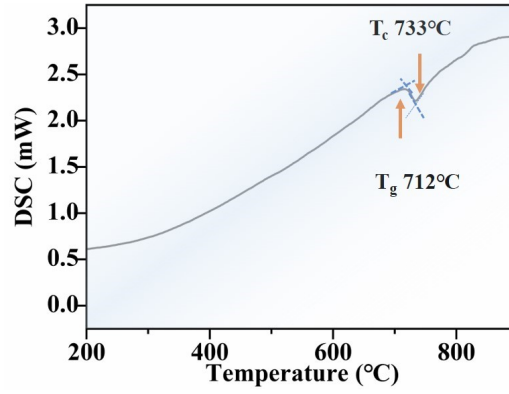


Figure S1 DSC curve of PG recorded at a heating rate of 10 K/min ( $T_g$  and  $T_c$  denotes the glass transition temperature and the onset crystallization temperature, respectively).

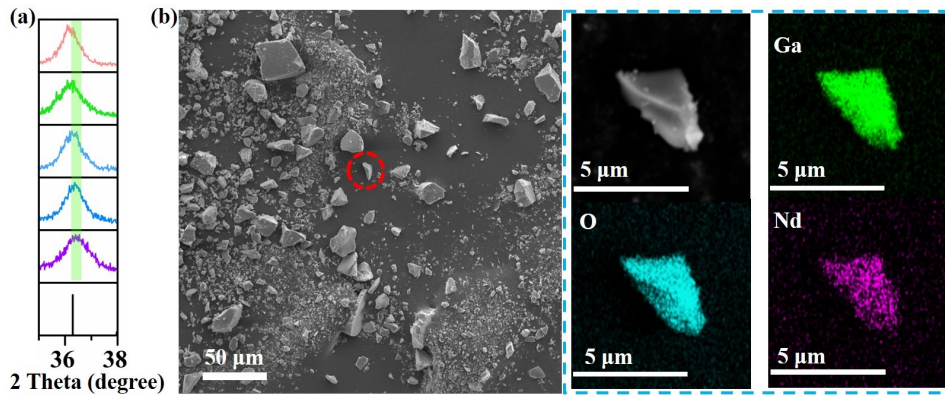


Figure S2 (a) XRD patterns of  $\text{LiGa}_5\text{O}_8: x\text{Nd}^{3+}$  GCs ( $x = 0.1, 0.15, 0.20, 0.25,$  and  $0.30$ ) in the region of  $35.5 - 38^\circ$ . (b) SEM image and the corresponding elemental mapping of  $\text{LiGa}_5\text{O}_8: \text{Nd}^{3+}$  GC.

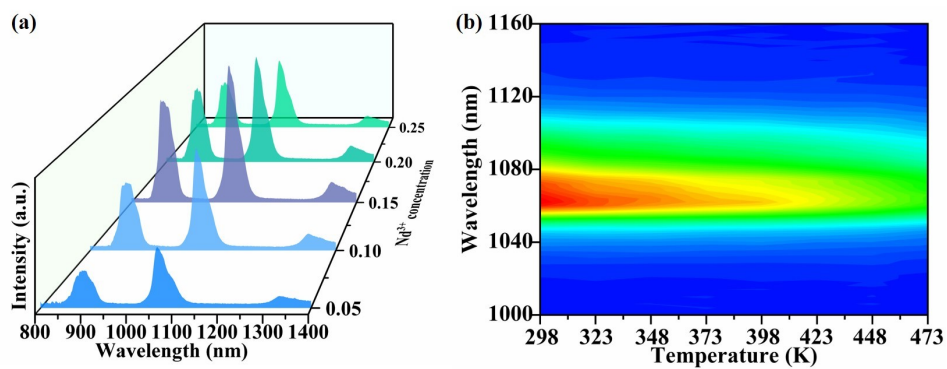


Figure S3 (a) PL spectra of  $\text{LiGa}_5\text{O}_8: x\text{Nd}^{3+}$  GC ( $x = 0.1, 0.15, 0.20, 0.25,$  and  $0.30$ ) dependent on the concentration of  $\text{Nd}^{3+}$  ions. (b) Temperature-dependent PL spectra ranging from RT to 473 K.

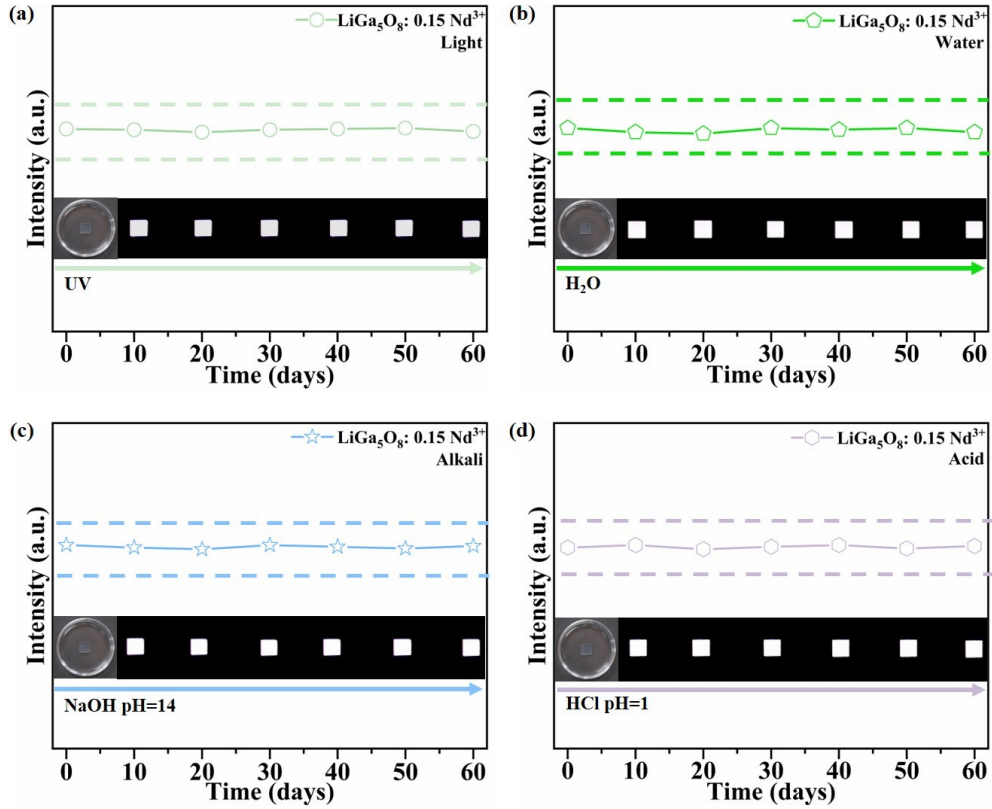


Figure S4 The integrated emission intensity of the  $\text{LiGa}_5\text{O}_8:0.15\text{Nd}^{3+}$  GCs recorded at continuous illumination by a 365 nm UV lamp (a), immersed in water (b), NaOH solution (c), and HCl solution (d) for prolonged recorded time, respectively. The insets in (a), (b), (c) and (d) is the corresponding photographs of the samples.

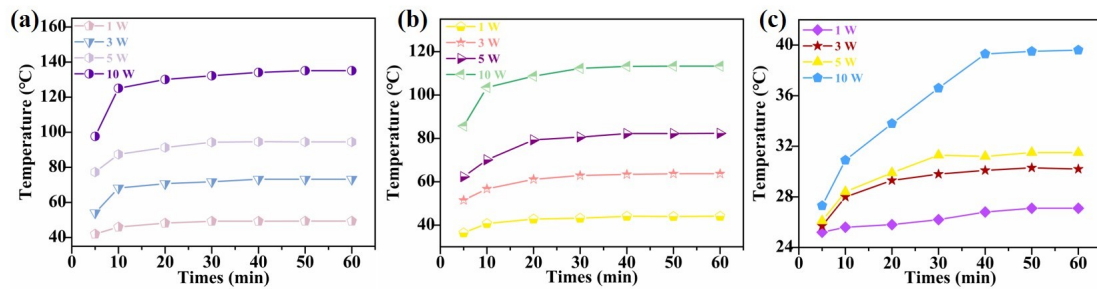


Figure S5 LED temperature recorded with the prolonged working time from 10 to 60 min with different driving current, (a) pc-LED, (b) GCs LED with contact packaging structure, (c) GCs LED with a hollow packaging structure.

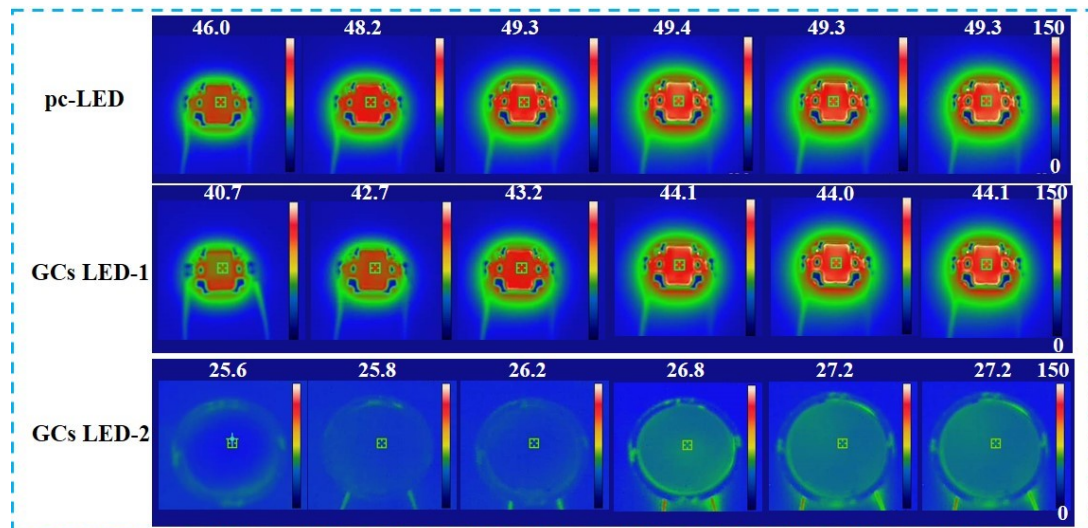


Figure S6 Thermal imaging of (a) pc-LED, (b) GCs LED-1, (c) GCs LED-2 recorded under the driving current of 0.3 A with the extension of the working time from 10 to 60 min.

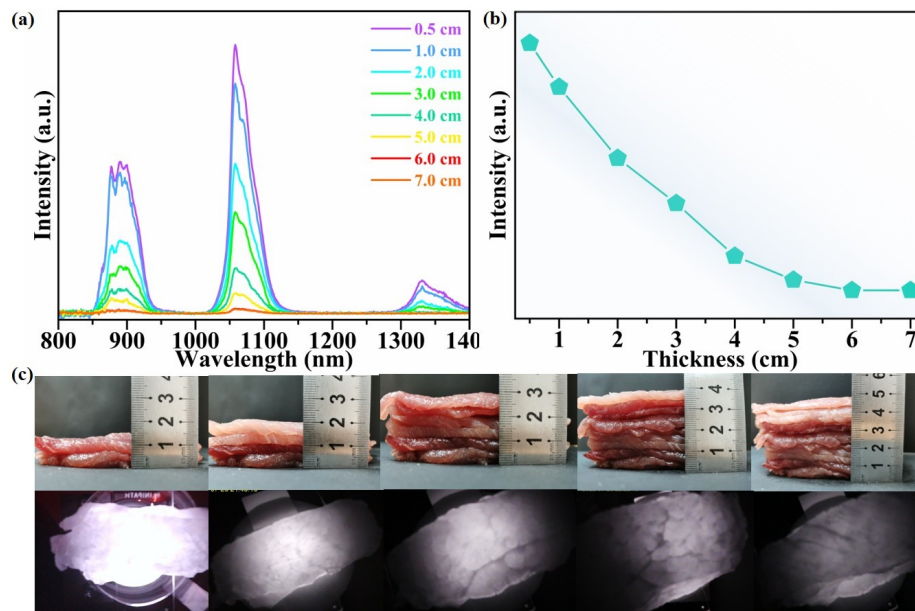


Figure S7 The luminescence spectra (a), and the corresponding plotted luminescence intensity (b) of the as-explored NIR LED recorded for the different penetration depth of pork tissue. (c) Photos of different pork tissue thickness under natural light and under the as-explored NIR light.